Forced convection in thermally developing turbulent flow of drag-reducing fluids within circular tubes

E.N. Macêdo [a], C.E. Maneschy [a], J.N.N. Quaresma [b],*

[a]*Mechanical Engineering Department — CT, Universidade Federal do Pará, Campus Universitário do Guamá, Rua Augusto Corrêa, 01 66075-900 Belém, PA, Brazil*
[b]*Chemical Engineering Department — CT, Universidade Federal do Pará, Campus Universitário do Guamá, Rua Augusto Corrêa, 01 66075-900 Belém, PA, Brazil*

Abstract

The Integral Transform Technique is used to solve the turbulent forced convection problem for drag-reducing fluids in the thermal developing and fully developed regions within circular tubes. Turbulent effects are taken into account through an algebraic model corresponding to the minimum-drag asymptotic case for viscoelastic fluids. The well-established Sign-Count Method and the Generalized Integral Transform Technique (GITT) are both employed in order to compute the eigenvalues and the respective eigenfunctions of the associated Sturm–Liouville problem. The Nusselt numbers calculated with the present approach are then compared with those obtained from experimental works available in the literature. © 2000 Elsevier Science Ltd. All rights reserved.

1. Introduction

The drag reduction phenomenon has been known for about five decades. In his pioneering study in this area, Toms [1] observed that for turbulent flow some fluids exhibited a smaller friction coefficient and smaller heat transfer rates than Newtonian fluids. However, in a recent paper, Kostic [2] pointed out that such phenomenon is not quite well understood, because the classical isotropic fluid mechanics is not applicable to very complex fluids and because the turbulence phenomenon is also not well understood, even for Newtonian fluids; so that many questions about these fluids remain unanswered.

Nowadays, there are a great number of practical en-

gineering problems that make use of these characteristics, among them are included the transportation of clay suspensions through extensive pipelines. In this application, polymeric solutions presenting this behavior are added to these suspensions, in order to reduce the pressure drop and, consequently, the cost of pumping. Another application involving these fluids concerns to the design of heat exchange devices, where a lower heat transfer rate is obtained when compared with the newtonian situation, and the performance of such equipment is improved. The present work is not concerned with technological and theoretical aspects of the drag reduction phenomenon, which are covered in details in the paper by Kostic [2] and in several other excellent references available in the literature [3–8].

Turbulent forced convection problems within circular tubes have been solved by different methods, mostly purely numerical techniques. In this paper, the integral transform technique is used to solve the

* Corresponding author.
E-mail address: quaresma@ufpa.br (J.N.N. Quaresma).

Nomenclature

C	velocity ratio
$D_h = 2r_w$	hydraulic diameter
$E_h(R)$	total eddy diffusivity of heat
f	Fanning friction factor
$\bar{f}_i$	transformed inlet condition defined by Eq. (16b)
$h(z)$	local heat transfer coefficient
j_h	heat transfer j factor
k	thermal conductivity
m	constant related to boundary conditions
N_i	normalization integral defined by Eq. (15)
$Nu(Z)$, Nu_∞	local and asymptotic Nusselt numbers, respectively
p	pressure field
Pr_a	apparent Prandtl number
q_w	wall heat flux
r_w	tube radius
r, R	radial coordinate, dimensional and dimensionless, respectively
R^+	dimensionless variable defined by Eq. (4f)
Re_a	apparent Reynolds number
$T(r,z)$	dimensional temperature distribution
T_i	inlet temperature
T_w	prescribed wall temperature
$u(r)$, $U(R)$	velocity distribution, dimensional and dimensionless, respectively
u_m, u_{max}	average flow and maximum velocities, respectively
u^+	dimensionless velocity defined by Eqs.

	(4c) and (4d)
$W(R)$	velocity profile defined by Eq. (3e)
y^+	dimensionless radial coordinate related to Eq. (4d)
z, Z	axial coordinate, dimensional and dimensionless, respectively

Greek symbols

α	fluid thermal diffusivity
ε_h	eddy diffusivity of heat
η	dummy variable related to integrals in Eqs. (11d) and (11e)
μ_i	eigenvalues of problem (13)
ν_a	apparent kinematic viscosity
ξ	dummy variable related to integral in Eq. (11d)
$\Psi_i(R)$	eigenfunctions of problem (13)
ρ	density
τ_w	wall shear stress
$\theta(R, Z)$	dimensionless temperature distribution
$\theta_{av}(Z)$	dimensionless average temperature
$\theta_h(R, Z)$	solution of homogeneous problem (12)
$\bar{\theta}_{hi}(Z)$	integral transform defined by Eq. (14a)
$\theta_p(R)$	solution of particular problem (11)

Subscripts and superscripts

av	related to average quantities
-	integral transform

heat transfer problem in both thermal developing and fully developed regions within a circular tube, involving drag-reducing fluids. Such precision-controlled technique has been used in the solution of different diffusion and convection diffusion problems [9,10]. In the application of this technique the related eigenvalue problem is solved through both the well-established Sign-Count Method [11] and the Generalized Integral Transform Technique (GITT) [10,12], permitting the determination of the eigenvalues and their respective eigenfunctions with accurate precision, as well as other related eigenquantities.

In this context, the Nusselt numbers are computed and compared with those obtained from empirical correlations and other works available in the literature [7,13,14]. Such results, as computed by the present approach, have their precision controlled by the num-

ber of eigenquantities utilized in the solution, as described next. The turbulent effects are taken into account by employing the turbulent velocity profile by Virk et al. [6], corresponding to the minimum-drag asymptotic case, and the algebraic model for the total eddy diffusivity of heat suggested by Cho and Hartnett [7].

2. Analysis

Steady-state heat transfer problem of an incompressible drag-reducing fluid flowing in both the thermal entry and fully-developed regions of a circular tube is analyzed. The flow is considered to be hydrodynamically developed; the wall tube is subjected either to a prescribed uniform heat flux or a prescribed constant temperature; and the fluid enters with a uniform tem-

perature, T_i. Axial diffusion, wall-conjugation and the viscous dissipation term in the energy equation are neglected, and the physical properties are assumed to be constant.

The mathematical formulation for this general forced convection heat transfer problem in dimensionless form is written as:

$$W(R)\frac{\partial\theta(R,Z)}{\partial Z} = \frac{\partial}{\partial R}\left[RE_h(R)\frac{\partial\theta(R,Z)}{\partial R}\right],$$

$$\text{in } 0 < R < 1, Z > 0 \tag{1a}$$

subjected to the inlet and boundary conditions

$$\theta(R,0) = 0, \quad 0 \le R \le 1 \tag{1b}$$

$$\left.\frac{\partial\theta(R,Z)}{\partial R}\right|_{R=0} = 0, Z > 0 \tag{1c}$$

$$(1-m)\theta(1,Z) + m\frac{\partial\theta(1,Z)}{\partial R} = 1, \quad Z > 0 \tag{1d}$$

where the constant "m" is related to the boundary conditions in the following form:

$$m = \begin{cases} 0 & \text{for prescribed wall temperature} \\ 1 & \text{for prescribed wall heat flux} \end{cases} \tag{2}$$

The following dimensionless groups were employed in Eqs. (1a)–(1d) above

$$R = \frac{r}{r_w} \tag{3a}$$

$$Z = \frac{4z/D_h}{C\,Re_a Pr_a} \tag{3b}$$

$$U(R) = \frac{u(r)}{u_{max}} \tag{3c}$$

$$C = \frac{u_{max}}{u_m} \tag{3d}$$

$$W(R) = RU(R) \tag{3e}$$

$$Re_a = \frac{u_m D_h}{\nu_a} \tag{3f}$$

$$Pr_a = \frac{\nu_a}{\alpha} \tag{3g}$$

$$E_h(R) = 1 + \frac{\varepsilon_h}{\alpha} = 1 + Pr_a\frac{\varepsilon_h}{\nu_a} \tag{3h}$$

and

$$\theta(R,Z) = \frac{T(r,z) - T_i}{T_w - T_i}, \tag{3i}$$

for prescribed wall temperature ($m = 0$)

$$\theta(R,Z) = \frac{T(r,z) - T_i}{(q_w r_w/k)}, \tag{3j}$$

for prescribed wall heat flux ($m = 1$)

where $D_h = 2r_w$ is the hydraulic diameter and Re_a and Pr_a are the apparent Reynolds and Prandtl numbers.

The turbulent dimensionless velocity profile, $U(R)$, and the algebraic model for the total eddy diffusivity of heat, $E_h(R)$, corresponding to the minimum-drag asymptotic case, are taken, respectively, from the works by Virk et al. [6], and Cho and Hartnett [7]:

$$U(R) = \frac{2}{C}\sqrt{\frac{f}{8}}u^+ \tag{4a}$$

$$E_h(R) = 1 + Pr_a\frac{\varepsilon_h}{\nu_a} \tag{4b}$$

$$u^+ = 11.7\ln\left((1-R)R^+\right) - 17.0, \quad R \le 1 - \frac{11.6}{R^+} \tag{4c}$$

$$u^+ = y^+ = (1-R)R^+, \quad R \ge 1 - \frac{11.6}{R^+} \tag{4d}$$

$$\frac{\varepsilon_h}{\nu_a} = 2.5 \times 10^{-6}\left(y^+\right)^3 = 2.5 \times 10^{-6}\left((1-R)R^+\right)^3 \tag{4e}$$

with

$$R^+ = Re_a\sqrt{\frac{f}{8}} \tag{4f}$$

The Fanning friction factor is defined as

$$f = \left(-\frac{dp}{dz}\right)\frac{D_h}{2\rho u_m^2} = \frac{\tau_w}{\frac{1}{2}\rho u_m^2} \tag{5}$$

which is computed by satisfying the equation for the average flow velocity, in the following form

$$4\sqrt{\frac{f}{8}}\int_0^1 Ru^+\,dR = 1 \tag{6}$$

The relation of velocities $C = u_{max}/u_m$ is obtained from Eqs. (4c) and (4d) resulting

$$C = 2\sqrt{\frac{f}{8}}(11.7 \ln(R^+) - 17.0) \tag{7}$$

Therefore, for a given apparent Reynolds number and friction factor f, C is readily determined from this expression.

Table 1 shows the comparison between the Fanning friction factor computed from the present analysis and the one found from the empirical correlation by Cho and Hartnett [7], with an excellent agreement being observed. The relation of velocity, C, is also shown in this table.

The problem defined by Eqs. (1) can be readily solved by the classical integral transform technique [9,10]. However, in order to obtain a convergence acceleration of the final solution, the so-called splitting-up procedure [9,15] is applied to this problem. Then, it is proposed as a general separation into simpler problems in the form:

$$\theta(R, Z) = m\theta_{av}(Z) + \theta_p(R) + \theta_h(R, Z) \tag{8}$$

where $\theta_{av}(Z)$ is the average temperature, defined as:

$$\theta_{av}(Z) = \frac{\int_0^1 W(R)\theta(R, Z)\,dR}{\int_0^1 W(R)\,dR} \tag{9}$$

and, for the case of a prescribed wall heat flux, when all boundary conditions are of the second kind, the average temperature is given a priori in the form:

$$\theta_{av}(Z) = \frac{Z}{\int_0^1 W(R)\,dR} = 2CZ \tag{10}$$

In Eq. (8), $\theta_p(R)$ represents the separated solution due to the nonhomogeneous boundary condition, Eq. (1d), and $\theta_h(R, Z)$ is the homogeneous version of problem (1), and are obtained from the following formulations:

Table 1
Fanning friction factor computed from the present analysis

Re_a	f		$C = u_{max}/u_m$
6000	0.003679353[a]	0.003072680[b]	1.70837642
10,000	0.002705998	0.002404529	1.61880314
60,000	0.001111937	0.001017460	1.40931996
100,000	0.0009016435	0.0007962143	1.36993435

[a] Present analysis.
[b] Empirical correlation proposed by Cho and Hartnett [7].

$$\frac{d}{dR}\left[RE_h(R)\frac{d\theta_p(R)}{dR} \right] - 2mCW(R) = 0, \tag{11a}$$
$$\text{in } 0 < R < 1$$

with boundary conditions

$$\left.\frac{d\theta_p(R)}{dR}\right|_{R=0} = 0 \tag{11b}$$

$$(1 - m)\theta_p(1) + m\left.\frac{d\theta_p(R)}{dR}\right|_{R=1} = 1 \tag{11c}$$

which is readily integrated to furnish

$$\theta_p(R) = (1 - m) + m\left\{ \theta_p(1) + 2C\int_1^R \left[\frac{\int_0^\eta W(\xi)\,d\xi}{\eta E_h(\eta)} \right]d\eta \right\} \tag{11d}$$

$$\theta_p(1) = 4C^2 \int_0^1 \frac{\left[\int_0^R W(\eta)\,d\eta \right]^2}{RE_h(R)}\,dR \tag{11e}$$

and, the general homogeneous problem is given by:

$$W(R)\frac{\partial \theta_h(R, Z)}{\partial Z} = \frac{\partial}{\partial R}\left[RE_h(R)\frac{\partial \theta_h(R, Z)}{\partial R} \right], \tag{12a}$$
$$\text{in } 0 < R < 1, Z > 0$$

$$\theta_h(R, 0) = -\theta_p(R), \quad 0 \le R \le 1 \tag{12b}$$

$$\left.\frac{\partial \theta_h(R, Z)}{\partial R}\right|_{R=0} = 0, \quad Z > 0 \tag{12c}$$

$$(1 - m)\theta_h(1, Z) + m\frac{\partial \theta_h(1, Z)}{\partial R} = 0, \quad Z > 0 \tag{12d}$$

The homogeneous problem given by Eqs. (12) can be solved by the classical integral transform technique [9,10]. Then, following the procedures of this technique, the general appropriate eigenvalue problem needed for its solution is taken as

$$\frac{d}{dR}\left[RE_h(R)\frac{d\Psi_i(R)}{dR} \right] + \mu_i^2 W(R)\Psi_i(R) = 0, \tag{13a}$$
$$\text{in } 0 < R < 1$$

$$\left.\frac{d\Psi_i(R)}{dR}\right|_{R=0} = 0 \tag{13b}$$

$$(1 - m)\Psi_i(1) + m\frac{\mathrm{d}\Psi_i(1)}{\mathrm{d}R} = 0 \qquad (13\mathrm{c})$$

where $\Psi_i(R)$ and μ_i are, respectively, the eigenfunctions and eigenvalues. The problem defined by Eqs. (13) is solved by the so-called Sign-Count Method [11] and Generalized Integral Transform Technique [10,12], which offer safe and automatic computations of as many eigenvalues and eigenfunctions as it is desired, with controlled accuracy. The eigenvalue problem above allows for the development of the following integral transform pair:

$$\bar{\theta}_{\mathrm{hi}}(Z) = \int_0^1 W(R)\Psi_i(R)\theta_{\mathrm{h}}(R, Z)\,\mathrm{d}R, \quad \text{transform} \qquad (14\mathrm{a})$$

$$\theta_h(R, Z) = \sum_{i=1}^{\infty} \frac{1}{N_i}\Psi_i(R)\bar{\theta}_{\mathrm{hi}}(Z), \quad \text{inversion} \qquad (14\mathrm{b})$$

where N_i is the normalization integral given by:

$$N_i = \int_0^1 W(R)\Psi_i^2(R)\,\mathrm{d}R \qquad (15)$$

Taking the integral transform of the system given by Eqs. (12), equations above are operated with $\int_0^1 \Psi_i(R)\,\mathrm{d}R$, and the following ordinary differential equation for the transformed potential, $\bar{\theta}_{\mathrm{hi}}(Z)$, is obtained

$$\frac{\mathrm{d}\bar{\theta}_{\mathrm{hi}}(Z)}{\mathrm{d}Z} + \mu_i^2\bar{\theta}_{\mathrm{hi}}(Z) = 0 \qquad (16\mathrm{a})$$

with the transformed inlet condition given by

$$\bar{\theta}_{\mathrm{hi}}(0) = \bar{f}_i = -\int_0^1 W(R)\Psi_i(R)\theta_{\mathrm{p}}(R)\,\mathrm{d}R \qquad (16\mathrm{b})$$

The solution for the transformed potential given by Eqs. (16) is readily obtained in the form

$$\bar{\theta}_{\mathrm{hi}}(Z) = \bar{f}_i \exp(-\mu_i^2 Z) \qquad (17)$$

Therefore, introducing Eq. (17) into the inversion formula (14b), the solution for $\theta_{\mathrm{h}}(R, Z)$ is determined as follows

$$\theta_{\mathrm{h}}(R, Z) = \sum_{i=1}^{\infty} \frac{\bar{f}_i}{N_i}\Psi_i(R)\exp(-\mu_i^2 Z) \qquad (18)$$

Thus, Eq. (18) in conjunction with Eqs. (11d) and (11e) for $\theta_{\mathrm{p}}(R)$ complete the solution for the potential $\theta(R, Z)$ defined in Eq. (8). This solution is written as:

$$\theta(R, Z) = m\theta_{\mathrm{av}}(Z) + (1 - m)$$

$$+ m\left\{\theta_{\mathrm{p}}(1) + 2C\int_1^R \frac{\left[\int_0^\eta W(\xi)\,\mathrm{d}\xi\right]}{\eta E_{\mathrm{h}}(\eta)}\,\mathrm{d}\eta\right\}$$

$$+ \sum_{i=1}^{\infty} \frac{\bar{f}_i}{N_i}\Psi_i(R)\exp(-\mu_i^2 Z) \qquad (19)$$

For the case of a prescribed wall heat flux ($m = 1$), the average temperature is given by Eq. (10). For the case of prescribed wall temperature ($m = 0$), when it is not determined a priori, it may be readily obtained by substituting the solution for $\theta(R, Z)$ (Eq. (19)) into Eq. (9) to yield:

$$\theta_{\mathrm{av}}(Z) = 1 + 2C\sum_{i=1}^{\infty} \frac{\bar{f}_i^2}{N_i}\exp(-\mu_i^2 Z) \qquad (20)$$

and the dimensionless wall heat flux is also determined from Eq. (19) as follows:

$$\left.\frac{\partial\theta(R, Z)}{\partial R}\right|_{R=1} = \sum_{i=1}^{\infty} \frac{\bar{f}_i}{N_i}\left.\frac{\mathrm{d}\Psi_i(R)}{\mathrm{d}R}\right|_{R=1}\exp(-\mu_i^2 Z)$$

$$= \sum_{i=1}^{\infty} \frac{\bar{f}_i^2\mu_i^2}{N_i}(-\mu_i^2 Z), \quad \text{for } m = 0 \qquad (21)$$

The local Nusselt number for both situations is defined as:

$$Nu(Z) = \frac{h(z)D_{\mathrm{h}}}{k} = \frac{2\left.\dfrac{\partial\theta(R, Z)}{\partial R}\right|_{R=1}}{\theta(1, Z) - \theta_{\mathrm{av}}(Z)} \qquad (22)$$

after substituting Eq. (21) for $\frac{\partial\theta(R,Z)}{\partial R}|_{R=1}$, and Eq. (20), for the case of a prescribed wall temperature, into Eq. (22) above, results:

$$Nu(Z) = \frac{\displaystyle\sum_{i=1}^{\infty} \frac{\bar{f}_i^2\mu_i^2}{N_i}\exp(-\mu_i^2 Z)}{C\displaystyle\sum_{i=1}^{\infty} \frac{\bar{f}_i^2}{N_i}\exp(-\mu_i^2 Z)} \qquad (23)$$

The asymptotic Nusselt number, Nu_∞, is obtained from Eq. (23) by considering only the first term in the summation, to yield:

$$Nu_\infty = \frac{\mu_1^2}{C} \qquad (24)$$

For the case of a prescribed wall heat flux the wall temperature $\theta(1, Z)$ is obained from Eq. (19) as:

$$\theta(1, Z) = \theta_{av}(Z) + \theta_p(1) + \sum_{i=1}^{\infty} \frac{\bar{f}_i}{N_i} \Psi_i(1)\exp\left(-\mu_i^2 Z\right) \qquad (25)$$

with,

$$\bar{f}_i = -\frac{\Psi_i(1)}{\mu_i^2} \qquad (26)$$

The local Nusselt number for this case is now completed by substituting Eqs. (25) and (26) into Eq. (22) resulting

Table 2
First 10 eigenvalues and $\bar{f}_i^2/N_i$ for various Reynolds and Prandtl numbers for the case of prescribed wall temperature

$m = 1$ (prescribed wall temperature)

Re_a	Pr_a	7.3			10.3		
	i	$\bar{f}_i^2/N_i$	μ_i[a]	μ_i[b]	$\bar{f}_i^2/N_i$	μ_i[a]	μ_i[b]
6×10^3	1	2.6949E−1	3.4678E+0	3.4678E+0	2.7239E−1	3.6059E+0	3.6059E+0
	2	1.3490E−2	1.2981E+1	1.2981E+1	1.1791E−2	1.4259E+1	1.4259E+1
	3	4.0000E−3	2.1626E+1	2.1626E+1	3.4979E−3	2.3790E+1	2.3790E+1
	4	1.7800E−3	3.0218E+1	3.0218E+1	1.5607E−3	3.3265E+1	3.3265E+1
	5	9.8000E−4	3.8776E+1	3.8776E+1	8.6120E−4	4.2700E+1	4.2699E+1
	6	6.1000E−4	4.7310E+1	4.7310E+1	5.4030E−4	5.2103E+1	5.2103E+1
	7	4.1000E−4	5.5823E+1	5.5823E+1	3.6880E−4	6.1480E+1	6.1480E+1
	8	3.0000E−4	6.4319E+1	6.4319E+1	2.6660E−4	7.0836E+1	7.0836E+1
	9	2.2000E−4	7.2800E+1	7.2800E+1	2.0080E−4	8.0177E+1	8.0176E+1
	10	1.7000E−4	8.1271E+1	8.1271E+1	1.5570E−4	8.9507E+1	8.9506E+1
1×10^4	1	2.9122E−1	3.8783E+0	3.8783E+0	2.9368E−1	4.0558E+0	4.0558E+0
	2	1.0220E−2	1.6953E+1	1.6953E+1	8.7745E−3	1.8819E+1	1.8819E+1
	3	3.0800E−3	2.8284E+1	2.8284E+1	2.6559E−3	3.1408E+1	3.1408E+1
	4	1.3700E−3	3.9568E+1	3.9568E+1	1.1838E−3	4.3957E+1	4.3957E+1
	5	7.5000E−4	5.0815E+1	5.0815E+1	6.5010E−4	5.6464E+1	5.6464E+1
	6	4.6000E−4	6.2033E+1	6.2033E+1	4.0560E−4	6.8937E+1	6.8937E+1
	7	3.1000E−4	7.3229E+1	7.3229E+1	2.7560E−4	8.1380E+1	8.1380E+1
	8	2.2000E−4	8.4403E+1	8.4403E+1	1.9880E−4	9.3797E+1	9.3797E+1
	9	1.7000E−4	9.5561E+1	9.5561E+1	1.4960E−4	1.0619E+2	1.0619E+2
	10	1.3000E−4	1.0670E+2	1.0670E+2	1.1630E−4	1.1857E+2	1.1857E+2
6×10^4	1	3.5006E−1	6.6743E+0	6.6743E+0	3.5084E−1	7.0492E+0	7.0492E+0
	2	2.5810E−3	5.7043E+1	5.7043E+1	2.1424E−3	6.4651E+1	6.4652E+1
	3	8.7900E−4	9.3707E+1	9.3707E+1	7.3610E−4	1.0598E+2	1.0599E+2
	4	4.0100E−4	1.3078E+2	1.3078E+2	3.3660E−4	1.4785E+2	1.4785E+2
	5	2.2000E−4	1.6794E+2	1.6794E+2	1.8530E−4	1.8984E+2	1.8985E+2
	6	1.3600E−4	2.0511E+2	2.0511E+2	1.1490E−4	2.3185E+2	2.3186E+2
	7	9.1000E−5	2.4227E+2	2.4227E+2	7.7400E−5	2.7384E+2	2.7385E+2
	8	6.5000E−5	2.7940E+2	2.7940E+2	5.5400E−5	3.1580E+2	3.1581E+2
	9	4.8000E−5	3.1650E+2	3.1650E+2	4.1500E−5	3.5772E+2	3.5773E+2
	10	3.7000E−5	3.5357E+2	3.5357E+2	3.2200E−5	3.9960E+2	3.9961E+2
1×10^5	1	3.6195E−1	8.0161E+0	8.0161E+0	3.6246E−1	8.4753E+0	8.4753E+0
	2	1.6250E−3	8.5243E+1	8.5243E+1	1.3434E−3	9.6923E+1	9.6925E+1
	3	5.7400E−4	1.3893E+2	1.3893E+2	4.7890E−4	1.5759E+2	1.5759E+2
	4	2.6500E−4	1.9345E+2	1.9345E+2	2.2160E−4	2.1929E+2	2.1929E+2
	5	1.4600E−4	2.4822E+2	2.4822E+2	1.2250E−4	2.8133E+2	2.8133E+2
	6	9.0000E−5	3.0307E+2	3.0307E+2	7.6100E−5	3.4347E+2	3.4348E+2
	7	6.1000E−5	3.5794E+2	3.5794E+2	5.1200E−5	4.0563E+2	4.0564E+2
	8	4.3000E−5	4.1279E+2	4.1279E+2	3.6600E−5	4.6777E+2	4.6778E+2
	9	3.2000E−5	4.6762E+2	4.6762E+2	2.7400E−5	5.2988E+2	5.2989E+2
	10	2.5000E−5	5.2241E+2	5.2241E+2	2.1200E−5	5.9194E+2	5.9196E+2

[a] Sign-Count Method.
[b] GITT approach.

$$Nu(Z) = \frac{2}{\theta_p(1) - \sum_{i=1}^{\infty} \dfrac{\Psi_i^2(1)}{N_i \mu_i^2} \exp\left(- \mu_i^2 Z\right)} \qquad (27)$$

$$Nu_\infty = \frac{2}{\theta_p(1)} \qquad (28)$$

where, $\theta_p(1)$ is given by Eqs. (11d) and (11e). The asymptotic Nusselt number, Nu_∞ is determined by making $Z \rightarrow \infty$ in Eq. (27), so that

3. Results and discussion

To complete the solution it is necessary to evaluate the eigenvalues, μ_i, the eigenfunctions, $\Psi_i(R)$ and nor-

Table 3
First 10 eigenvalues and $\Psi_i^2(1)/N_i$ for various Reynolds and Prandtl numbers for the case of prescribed wall heat flux

$m = 1$ (prescribed wall heat flux)

Re_a	Pr_a	7.3			10.3		
	i	$\Psi_i^2(1)/N_i$	$\mu_i{}^a$	$\mu_i{}^b$	$\Psi_i^2(1)/N_i$	$\mu_i{}^a$	$\mu_i{}^b$
6×10^3	1	1.1936E+1	9.5808E+0	9.5808E+0	1.3520E+1	1.0575E+1	1.0575E+1
	2	1.2391E+1	1.8579E+1	1.8579E+1	1.4087E+1	2.0463E+1	2.0463E+1
	3	1.3668E+1	2.7283E+1	2.7283E+1	1.5592E+1	3.0044E+1	3.0044E+1
	4	1.4927E+1	3.5878E+1	3.5878E+1	1.7052E+1	3.9506E+1	3.9506E+1
	5	1.6066E+1	4.4415E+1	4.4415E+1	1.8337E+1	4.8907E+1	4.8907E+1
	6	1.7050E+1	5.2921E+1	5.2921E+1	1.9411E+1	5.8275E+1	5.8275E+1
	7	1.7875E+1	6.1410E+1	6.1410E+1	2.0290E+1	6.7627E+1	6.7627E+1
	8	1.8561E+1	6.9890E+1	6.9890E+1	2.1019E+1	7.6972E+1	7.6972E+1
	9	1.9145E+1	7.8366E+1	7.8366E+1	2.1658E+1	8.6315E+1	8.6315E+1
	10	1.9668E+1	8.6841E+1	8.6841E+1	2.2262E+1	9.5656E+1	9.5656E+1
1×10^4	1	1.6034E+1	1.2520E+1	1.2520E+1	1.8264E+1	1.3996E+1	1.3996E+1
	2	1.6233E+1	2.4290E+1	2.4290E+1	1.8646E+1	2.7017E+1	2.7017E+1
	3	1.7787E+1	3.5733E+1	3.5733E+1	2.0518E+1	3.9719E+1	3.9719E+1
	4	1.9385E+1	4.7039E+1	4.7039E+1	2.2421E+1	5.2275E+1	5.2275E+1
	5	2.0885E+1	5.8273E+1	5.8273E+1	2.4165E+1	6.4751E+1	6.4751E+1
	6	2.2234E+1	6.9462E+1	6.9462E+1	2.5689E+1	7.7180E+1	7.7180E+1
	7	2.3412E+1	8.0624E+1	8.0624E+1	2.6979E+1	8.9583E+1	8.9583E+1
	8	2.4419E+1	9.1770E+1	9.1770E+1	2.8057E+1	1.0197E+2	1.0197E+2
	9	2.5275E+1	1.0291E+2	1.0291E+2	2.8970E+1	1.1435E+2	1.1435E+2
	10	2.6013E+1	1.1404E+2	1.1404E+2	2.9776E+1	1.2673E+2	1.2673E+2
6×10^4	1	5.7591E+1	4.3266E+1	4.3266E+1	6.6202E+1	4.9523E+1	4.9524E+1
	2	5.6217E+1	8.0608E+1	8.0608E+1	6.5756E+1	9.1407E+1	9.1408E+1
	3	6.0608E+1	1.1817E+2	1.1817E+2	7.1271E+1	1.3374E+2	1.3375E+2
	4	6.5609E+1	1.5557E+2	1.5557E+2	7.7477E+1	1.7595E+2	1.7595E+2
	5	7.0510E+1	1.9286E+2	1.9286E+2	8.3500E+1	2.1803E+2	2.1804E+2
	6	7.5173E+1	2.3004E+2	2.3004E+2	8.9139E+1	2.6002E+2	2.6002E+2
	7	7.9531E+1	2.6716E+2	2.6716E+2	9.4294E+1	3.0192E+2	3.0193E+2
	8	8.3536E+1	3.0422E+2	3.0422E+2	9.8910E+1	3.4378E+2	3.4379E+2
	9	8.7162E+1	3.4124E+2	3.4124E+2	1.0298E+2	3.8560E+2	3.8561E+2
	10	9.0403E+1	3.7823E+2	3.7823E+2	1.0653E+2	4.2739E+2	4.2739E+2
1×10^5	1	8.7355E+1	6.5236E+1	6.5236E+1	1.0061E+2	7.4900E+1	7.4902E+1
	2	8.4702E+1	1.1966E+2	1.1966E+2	9.9327E+1	1.3611E+2	1.3612E+2
	3	9.1058E+1	1.7485E+2	1.7485E+2	1.0736E+2	1.9845E+2	1.9846E+2
	4	9.8465E+1	2.2997E+2	2.2997E+2	1.1659E+2	2.6080E+2	2.6081E+2
	5	1.0575E+2	2.8499E+2	2.8499E+2	1.2561E+2	3.2305E+2	3.2306E+2
	6	1.1272E+2	3.3992E+2	3.3992E+2	1.3411E+2	3.8522E+2	3.8523E+2
	7	1.1927E+2	3.9476E+2	3.9476E+2	1.4196E+2	4.4729E+2	4.4731E+2
	8	1.2535E+2	4.4954E+2	4.4954E+2	1.4907E+2	5.0931E+2	5.0932E+2
	9	1.3091E+2	5.0427E+2	5.0427E+2	1.5541E+2	5.7128E+2	5.7130E+2
	10	1.3594E+2	5.5895E+2	5.5895E+2	1.6100E+2	6.3321E+2	6.3321E+2

[a] Sign-Count Method.
[b] GITT Approach.

malization integral, N_i, of the eigenvalue problem (13), as well as, other related eigenquantities. In this paper, the sign-count method [11] and the generalized integral transform technique [10,12] were used to determine these quantities, which, in turn, are necessary to compute the average temperature and the local Nusselt number from Eqs. (20), (23) and (27), respectively.

Tables 2 and 3 show the results obtained through the two approaches cited above, which are in perfect agreement. Due to space limitations, only the first ten eigenquantities are listed for various Reynolds and Prandtl numbers and for the two cases of boundary conditions at the wall tube adopted here.

Fig. 1 shows the evolution of the local Nusselt number as a function of the coordinate Z, in the thermal entry region, for both situations studied here, i.e., prescribed wall temperature and prescribed wall heat flux. The Reynolds and Prandtl numbers considered were, respectively, $Re_a = 15,100$ and $Pr_a = 7.01$. The analysis permits the comparison among the results from the present work and those predicted by the empirical correlations of Toh and Ghajar [13] and Yoo et al. [14], which were developed for the case of uniform wall heat flux and are, respectively, given by

$$j_h = 0.15\left(\frac{z}{D_h}\right)^{-0.29} Re_a^{-0.43}, \quad 10 < \frac{z}{D_h} < 600 \qquad (29)$$

$$j_h = 0.093\left(\frac{z}{D_h}\right)^{-0.34} Re_a^{-0.36}, \quad 5 < \frac{z}{D_h} < 1100 \qquad (30)$$

and in terms of Nusselt number

$$Nu = 0.15\left(\frac{z}{D_h}\right)^{-0.29} Re_a^{0.57} Pr_a^{1/3},$$

$$10 < \frac{z}{D_h} < 600 \qquad (31)$$

$$Nu = 0.093\left(\frac{z}{D_h}\right)^{-0.34} Re_a^{0.64} Pr_a^{1/3},$$

$$5 < \frac{z}{D_h} < 1100 \qquad (32)$$

Fig. 2 brings a similar analysis for the case of $Re_a = 55,700$ and $Pr_a = 11.29$. The restriction $10 < (z/D_h) < 600$ of the empirical correlation proposed by Toh and Ghajar [13] implies that the results can be compared over the following ranges of Z:

$Re_a = 15,100$; $Pr_a = 7.01$:

$$2.43 \times 10^{-4} < Z < 1.46 \times 10^{-2}$$

$Re_a = 55,700$; $Pr_a = 11.29$:

$$4.49 \times 10^{-5} < Z < 2.70 \times 10^{-3}$$

In this paper, we investigated the Nusselt number over the range of $3 \times 10^{-4} < Z < 1.46 \times 10^{-2}$ for $Re_a = 15,100$ and $Pr_a = 7.01$, and over the range of $1 \times 10^{-4} < Z < 2.70 \times 10^{-3}$ for $Re_a = 55,700$ and $Pr_a = 11.29$. From these figures reasonable agreements are observed for the results found from this analysis and the empirical correlations pointed out above. Better results are depicted by comparing the case of prescribed wall heat flux with the empirical correlation by Toh and Ghajar [13], which predicts results with a maximum deviation of 17% for the case $Re_a = 15,100$ and $Pr_a = 7.01$ and of 14% for $Re_a = 55,700$ and

Fig. 1. Comparison of the local Nusselt number for $Re_a = 15,100$ and $Pr_a = 7.01$.
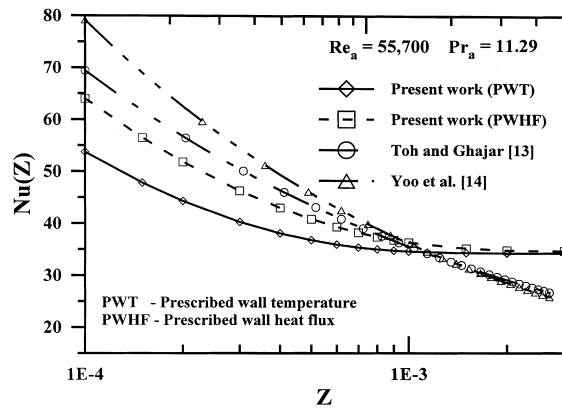

Fig. 2. Comparison of the local Nusselt number for $Re_a = 55,700$ and $Pr_a = 11.29$.
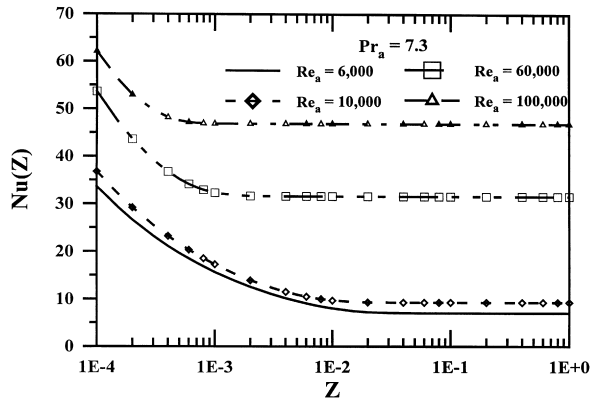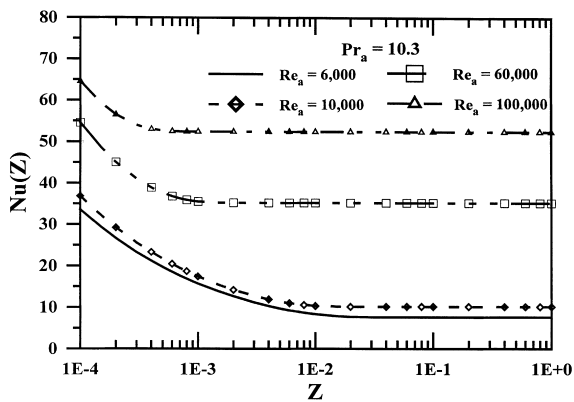
Fig. 3. Local Nusselt number in the thermal entry region for $Pr_a = 7.3$ and different Reynolds numbers for the case of prescribed wall temperature.
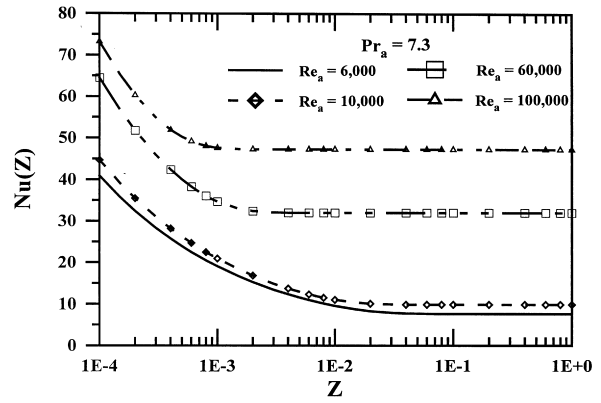

Fig. 5. Local Nusselt number in the thermal entry region for $Pr_a = 7.3$ and different Reynolds numbers for the case of prescribed wall heat flux.

$Pr_a = 11.29$. A maximum deviation of 38% is encountered for the case of prescribed wall temperature in relation to the empirical correlation presented by Yoo et al. [14] for $Re_a = 15,100$ and $Pr_a = 7.01$; and a maximum deviation of 31% for $Re_a = 55,700$ and $Pr_a = 11.29$. Higher deviations for the case of prescribed wall temperature can be justified by the fact that the experiments carried out by the investigators above were performed under constant wall heat flux. It can also be observed that when the coordinate Z increases the Nusselt numbers obtained from the present analysis reach asymptotic values, while the empirical correlations used for comparison can not predict asymptotic values of Nusselt numbers.

In Figs. 3 and 4 the Nusselt numbers $Nu(Z)$ obtained from the present calculation, plotted against Z, are shown along the thermal entry region, for four different Reynolds numbers (i.e., 6×10^3, 10^4, 6×10^4,

10^5) at $Pr_a = 7.3$ and 10.3, for the case of prescribed wall temperature. From these figures it can be noticed that the Nusselt number increases with an increase in the Reynolds and Prandtl numbers. It is also observed that the length of the thermal entry region decreases with increasing Reynolds number, for a fixed value of Prandtl number, i.e., the thermally developed region is reached more rapidly at higher Reynolds numbers.

Figs. 5 and 6 present a similar analysis for the case of a prescribed wall heat flux. The local Nusselt number, starting from the thermal entry region, decreases continuously with axial position until the fully-developed thermal region is reached. In this region, the local Nusselt number is represented by an asymptotic value. It is also noticed that the Nusselt numbers for the case of prescribed wall heat flux are slightly larger than those for the case of prescribed wall temperature.

Fig. 4. Local Nusselt number in the thermal entry region for $Pr_a = 10.3$ and different Reynolds numbers for the case of prescribed wall temperature.
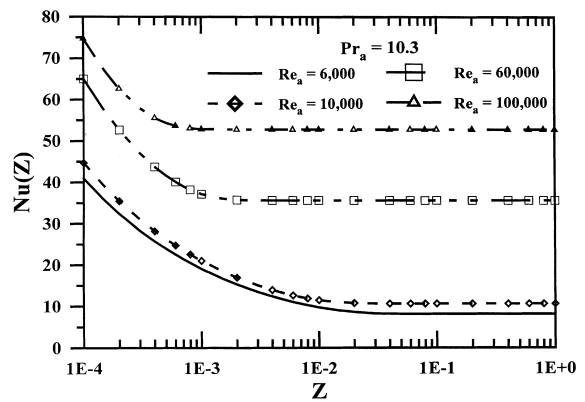

Fig. 6. Local Nusselt number in the thermal entry region for $Pr_a = 10.3$ and different Reynolds numbers for the case of prescribed wall heat flux.

Table 4
Asymptotic Nusselt number calculated from the present analysis

Re_a	$Pr_a = 7.3$		$Pr_a = 10.3$	
6000	7.0391[a]	7.6135[b]	7.6110[a]	8.1517[b]
10,000	9.2915	9.8338	10.162	10.670
60,000	31.608	32.030	35.260	35.653
100,000	46.906	47.296	52.437	52.799

[a] Prescribed wall temperature.
[b] Prescribed wall heat flux.

These observations are the same verified for the case of prescribed wall temperature.

For the values of Nusselt numbers plotted in Figs. 3–6 within the range of axial positions studied here a truncation order $N \leq 100$ in the simulations was required for full convergence, for all cases.

Finally, Table 4 shows a set of benchmark results for the asymptotic Nusselt number as a function of the Reynolds and Prandtl numbers for both cases studied here; prescribed wall temperature and prescribed wall heat flux. It can be noticed that a good agreement exists between these two sets of result. This good agreement confirms the evidence that in the fully-developed thermal region, when we adopt different boundary conditions in turbulent flow, there is not a strong influence in the results obtained.

4. Conclusions

The problem of turbulent convective heat transfer along the thermal entry and fully-developed flow regions of drag-reducing fluids with different boundary conditions at the tube wall has been analyzed, with excellent computational performance obtained through the classical integral transform technique. The well-established Sign-Count Method and GITT approach were used to calculate the related eigenvalue problems demonstrating excellent agreement in the results of the eigenquantities. Benchmark results were tabulated and graphically presented for different apparent Reynolds and Prandtl numbers. Results for the local Nusselt numbers along the thermal entry region were confronted with those from empirical correlations and a good agreement among them was verified for the case of prescribed wall heat flux.

References

[1] B.A. Toms, Some observations on the flow of linear polymer solutions through straight tubes at large Reynolds numbers, in: Proceedings of the 1st International Congress on Rheology, 2, North Holland, Amsterdam, 1949, pp. 135–141.

[2] M. Kostic, On turbulent drag and heat transfer reduction phenomena and laminar heat transfer enhancement in non-circular duct flow of certain non-Newtonian fluids, Int. J. Heat Mass Transfer 37 (suppl. 1) (1994) 133–147.

[3] D.W. Dodge, A.B. Metzner, Turbulent flow of non-newtonian systems, AIChE Journal 5 (1959) 189–204.

[4] A.B. Metzner, Heat transfer in non-Newtonian fluids, Advances in Heat Transfer 2 (1965) 357–397.

[5] J.L. Lumley, Drag reduction by additives, Annual Reviews of Fluid Mechanics 1 (1969) 367–384.

[6] P.S. Virk, H.S. Mickley, K.A. Smith, The ultimate asymptote and mean flow structure in Toms' phenomenon, Trans. ASME, J. Appl. Mech 37 (1970) 488–493.

[7] Y.I. Cho, J.P. Hartnett, Non-Newtonian fluids in circular pipe flow, Advances in Heat Transfer 15 (1982) 59–141.

[8] J.P. Hartnett, Viscoelastic fluids: a new challenge in heat transfer, the 1990 Max Jakob memorial award lecture, J. Heat Transfer 114 (1992) 296–303.

[9] M.D. Mikhailov, M.N. Özisik, Unified Analysis and Solutions of Heat and Mass Diffusion, Wiley, New York, 1984.

[10] R.M. Cotta, Integral Transforms in Computational Heat and Fluid Flow, CRC Press, Boca Raton, 1993.

[11] M.D. Mikhailov, N.L. Vulchanov, Computational procedure for Sturm–Liouville problems, J. Comp. Phys 50 (1983) 323–336.

[12] M.D. Mikhailov, R.M. Cotta, Integral transform method for eigenvalue problem, Commun. Numer. Methods Eng 10 (1994) 827–835.

[13] K.H. Toh, A.J. Ghajar, Heat transfer in the thermal entrance region for viscoelastic fluids in turbulent pipe flow, Int. J. Heat Mass Transfer 31 (1988) 1261–1267.

[14] S.S. Yoo, T.S. Hwang, C.S. Eum, S.C. Bae, Turbulent heat transfer of polyacrylamide solutions in the thermal entrance region of circular tube flows, Int. J. Heat Mass Transfer 36 (1993) 365–370.

[15] M.D. Mikhailov, Splitting up of heat-conduction problems, Letters Heat Mass Transf 4 (1977) 163–166.